University of Zawia Journal of Engineering Sciences and Technology (UZJEST)
Volume 4, Issue 2, (2026), pp 190-209, ISSN 3006-2764

Global MPPT of Photovoltaic Systems Under Partial Shading Conditions Using a Rank Charged System Search Algorithm

Aseel Khalid [1], Ali Albabeli [2], Hamzah Naji*[1]

[1] General Directorate of Education in Baghdad Al-Karkh 1, Iraqi Ministry of Education, Baghdad, Iraq.

[2] Mechatronics Engineering Department, College of Engineering, University of Mosul, Mosul, Iraq,

*Corresponding author email: bcc0041@mtu.edu.iq

Received: 30-08-2026 | Accepted: 06-11-2026 | Available online: 08-11-2026 | DOI:10.26629/uzjest.2026.15

ABSTRACT

Partial shading conditions (PSC) represent a very strong competitive PV system with many local peaks on the Power-Voltage (P-V) characteristic curves, and traditional Maximum Power Point Tracking (MPPT) algorithms may not be able to track maximum power point under standby mode. To address this challenge, we propose a new ultra-efficient maximum power point tracking (MPPT) framework using the newly developed Rank Charged System Search algorithm called CSSRank-MPPT in this paper. The new method combines principles for electrostatic interaction with a rank-based dynamic particle reduction strategy, roulette wheel selection and adaptive mutation based on some rank. Notably, a new convergence lock-in mechanism is integrated in to the controller framework and so it can terminate steady-state power fluctuations when reaching the Global Maximum Power Point (GMPP). By simulating the CSSRank-MPPT algorithm in MATLAB/Simulink under dynamically changing partial shading scenarios, it is shown that not only true GMPP can be tracked, but also convergence speed of less than 1.0 s, tracking efficiency above 99.8 percent and zero steady-state power-loss have been accomplished. Comparisons show that the CSSRank-MPPT method outperforms standard PSO and GWO algorithms in terms of convergence reliability and dynamic robustness.

Keywords: Maximum Power Point Tracking (MPPT); Photovoltaic Systems; Partial Shading Conditions (PSC); Rank Charged System Search (CSSRank); Metaheuristic Optimization.

تتبع نقطة القدرة القصوى الشامل لأنظمة الخلايا الكهروضوئية في ظل ظروف التظليل الجزئي باستخدام خوارزمية بحث النظام المشحون بالرتبة

أصيل خالد[1]، علي عبدالجبار[2]، حمزه ناجي*[1]

[1] المديرية العامة لتربية بغداد الكرخ الأولى، وزارة التربية العراقية، بغداد، العراق

[2] قسم هندسة الميكاترونكس، كلية الهندسة، جامعة الموصل، الموصل، العراق

ملخـــــص البحـــــث

تُشكّل ظروف التظليل الجزئي تحديًا كبيرًا لأنظمة الخلايا الكهروضوئية، إذ تُؤدي إلى ظهور قمم محلية متعددة على

"Articles published in *Univ Zawia J Eng Sci Technol* are licensed under a Creative Commons Attribution-NonCommercial 4.0 International License."

منحنيات خصائص القدرة–الجهد، مما يُفقد خوارزميات تتبع نقطة القدرة القصوى التقليدية فعاليتها. وللتغلب على هذا القيد، تُقدّم هذه الورقة البحثية إطار عمل جديدًا عالي الكفاءة لتتبع نقطة القدرة القصوى، يعتمد على خوارزمية البحث عن النظام المشحون رتبةً، والتي طُوّرت حديثًا، ويُطلق عليها اسم CSSRank-MPPT. يدمج الأسلوب المقترح مبادئ التفاعل الكهروستاتيكي مع استراتيجية ديناميكية لتقليل الجسيمات قائمة على الرتبة، واختيار عجلة الروليت، ومُعامل طفرة تكيفي قائم على الرتبة. والأهم من ذلك، تم دمج آلية قفل تقارب جديدة في بنية وحدة التحكم للقضاء على تذبذبات القدرة في حالة الاستقرار بمجرد الوصول إلى نقطة القدرة القصوى العالمية. في محاكاة باستخدام MATLAB/Simulink في ظل سيناريوهات التظليل الجزئي الديناميكي، نجح خوارزمية CSSRank–MPPT في تتبع نقطة الطاقة القصوى العالمية (GMPP) الحقيقية بسرعة تقارب فائقة (أقل من 1.0 ثانية)، وكفاءة تتبع عالية (أكثر من 99.8%)، وانعدام فقد الطاقة في الحالة المستقرة. وتُظهر المقارنة تفوق خوارزمية CSSRank–MPPT على خوارزميتي PSO وGWO القياسيتين من حيث موثوقية التقارب والمتانة الديناميكية.

الكلمات الدالة: تتبع نقطة القدرة القصوى؛ الأنظمة الكهروضوئية؛ ظروف التظليل الجزئي؛ خوارزمية بحث النظام المشحون؛ خوارزميات التحسين.

1. Introduction

Most Solar PV energy has emerged as one of the most vital clean energy sources globally. However, the non-linear current-voltage ($I-V$) and P-V output characteristics of PV modules depend heavily on solar irradiance and ambient temperature[1, 2]. Using a DC-DC power converter to extract as much power of system depends on the implementation of MPPT controller that can produce continuously maximum output due to variation in environmental conditions [3-5]. The curve with uniform solar irradiation possesses a peculiar MPP [6], To be precise, assumption standard deterministic methods — Perturb and Observe[7, 8] or Incremental Conductance [9]—can track with no effort. Nevertheless, the actual installations revealed that partial shading at PV strings takes place due to clouds, trees and nearest structures [10-12]. So, this leads to the presence of multiple Local MPP (LMPPs) and a single GMPP which constructs complex curves as shown in[13, 14]. Thus, conventional MPPT techniques tend to be stuck at these LMPPs resulting in significant power loss [15-17]. Physically the reason is that shaded solar cells become reverse-biased, so they fire up parallel bypass diodes to protect against thermal hot-spot damage; broken and fragments the P-V characteristic into a false multi-modal landscape with power losses from 30% to more than 70%, if local peaks mistaken for global peak. For this reason, the key goal of more sophisticated photovoltaic tracking control engineering is to create an intelligent global tracker which can handle complicated multi-peak curves quickly without causing converter switching stress or steady state energy dissipation. The PSC challenge is addressed using nature inspired metaheuristic algorithms such as Particle Swarm Optimization (PSO)[18], Cuckoo Search [19], Flower Pollination Algorithm (FPA)[20], and Grey Wolf Optimization (GWO); these methods have been extensively investigated [21]. While very efficient, most standard metaheuristics have two major disadvantages in PV MPPT applications: (1) severe steady-state power oscillation around the GMPP if stochastic perturbations are continued [22] , and (2) premature convergence to local peaks due to poor exploration-exploitation balance. An advanced physics-based optimizer called Rank Charged System Search (CSSRank) was recently introduced [23].CSSRank is a reduction of electrostatic force laws and dynamic ranks (which can be used by ranking agents)($Sel_{(it)}$) and adaptive mutation as well. This paper proposes the first successful adaptation of CSSRank to PV MPPT (CSSRank-MPPT). The proposed controller ensures fast GMPP determination with zero steady-state power losses during complicated partial shading conditions introducing a dedicated state-machine execution template and a convergence lock-in

mechanism. In contrast to traditional bio-inspired swarm optimizers based on heuristic social rules that use a constant search agent count across the entire tracking cycle, the proposed CSSRank-MPPT brings additional value by employing deterministic Coulomb and Gauss electrostatic force laws paired with dynamic rank-based particle pruning to remove unnecessary converter evaluations from consideration in later iterations. The single-diode model (Figure 1) is a widely used equivalent circuit to describe the electrical performance of PV cells under solar irradiance. The model is composed of a parallel connection of a photo-generated current source, along with the semiconductor diode and shunt resistance, to which series resistance model (internal bulk plus contact losses) and an open-circuit voltage are added. This simple circuit extracts the non-linear relationship between terminal voltage and corresponding output current and represents a theoretical model for solar array performance as a function of ever-changing environmental conditions.

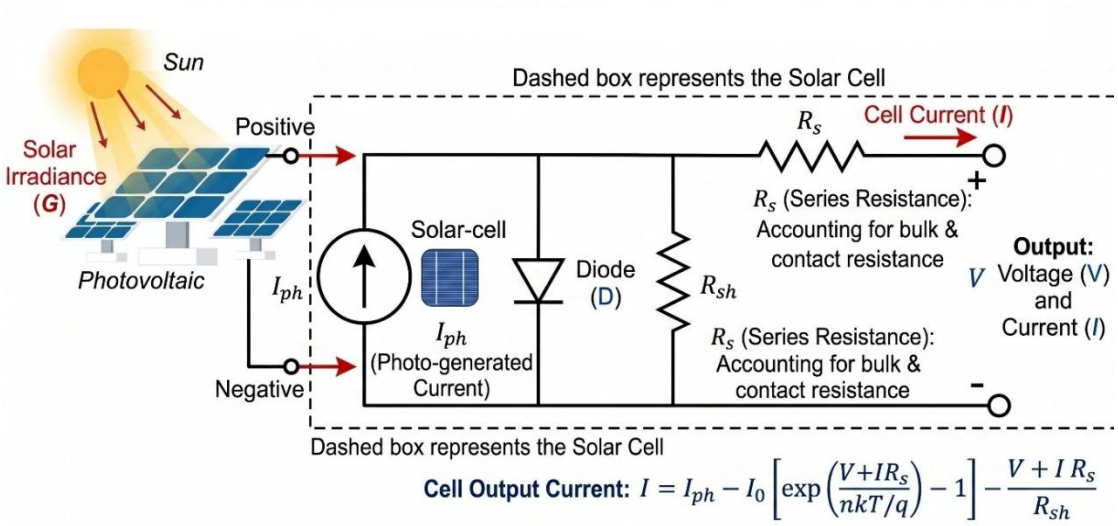


Figure 1. Single-Diode Equivalent Circuit Model of a Photovoltaic Solar Cell

Although metaheuristic algorithms, such as PSO and FPA, are widely employed for PV MPPT under PSC, these techniques have been impeded by persistent steady-state power oscillations around the global peak, alongside a high possibility of being prematurely stuck at local peaks. While Benchmark problems have previously demonstrated that the Rank-Based Charged System Search Algorithm (CSSRank) algorithm alleviates computational overhead and local optima trapping, this approach has never been adapted or reformulated to PV MPPT applications. Besides, conventional metaheuristics do not have an embedded lock-in approach to fix the duty cycle D in the identified maximum power point P, which keeps incurring energy losses continuously. As such, it unveils a distinct research gap in the development of an exclusive CSSRank-MPPT structure that reformulates electrostatic charge interplays for DC-DC converter duty cycle management while assuring fast global peak identification, steady-state power oscillation annihilation and dynamic re-tracking amidst instant irradiance fluctuations. Over the last decades, a lot of effort has been devoted to design high-performing MPPT algorithms in order to avoid power losses as much as possible due to PSC (Partial Shading Condition) and (Non-uniform irradiance). In the PSC, not a single point exists but there are some local maxima if you will see the power–voltage (PV) curves so traditional gradient-based trackers become inefficient. To provide a foundational perspective. Zheng et al. In [24], an improved elk herd optimization (IEHO) algorithm that includes predation risk avoidance, triangle walks, and redirection based on memory was proposed, which achieves an average tracking efficiency of 99.99%. For example, Hu and Ukil [25] presented an auxin and wither mechanism combination optimization (AWMCO) strategy that provided features for adaptive step sizes combined with the theoretical Lyapunov convergence guarantee. Similarly, Wang et al. Zhu et al. [26] improved the RIME optimization algorithm (IRIME) by adding logistic and piecewise chaotic

mappings with adaptive inertia weights to effectively balance global exploration versus local exploitation. Yet, careful consideration exposes profound conceptual shortcomings in these bio-inspired and chaotic paradigms: multi-stage behavioral updates like those applied in IEHO linearly exacerbate per-iteration computational burden; biological decay parameters present in AWMCO necessitate fine tuning for individual PV array sizes; and iterative perturbations generated from chaotic mapping sequences can still yield micro-oscillatory steps about the MPP before full cessation as reflected in IRIME. Specialized tracking frameworks have also been widely explored for control robustness and convergence acceleration. Alshareef [27]developed a modified WSO algorithm called Rank-Based Adaptive Weighted WSO by using adaptive rank weighting mechanism and bi-phase tactics. Kaaitan et al. Adedayo et al. in [28] used bio-inspired sooty tern optimization algorithm on a 3kW PV array which showed high tracking stability and less fluctuation of power output. Celikel et al. [29] proposed an enhanced GWO method, which limits the boundary search space after a few initial iterations resulting in three times faster tracking. Although the search convergence of these tracking strategies is accelerated, they keep a constant population size entire the search process, when forcing the DC-DC converter to perform unnecessary action-duty cycle evaluations by weak, low-fitness agents in a population already clustered around the global peak; furthermore, pre-mature boundary space restriction risks missing the actual GMPP occurrence with sudden changing incident solar irradiance levels during searching. Alhusseini et al. [30] the model predictive control combined with hybrid adaptive PSO Algorithm for optimal placement of distributed generation without PI loops and better dynamic response. In the context of structural single-variable optimization, Lee et al. In reference [31], an improved parameter-setting-free harmony search algorithm with a reduced-range operator was presented to also completely remove the overhead associated with tuning parameters and, moreover, reducing the converter current stresses. However, the combinations of metaheuristics with model predictive control adds large computational effort and converter parameters sensitivity, while under heavy shading, harmony search tracks slowly; furthermore, previous studies to the best of our knowledge mostly investigate a single converter without a hard duty-cycle freeze. Our work uniquely addresses this gap by adapting CSSRank electrostatic laws for a 0.10 to 0.90 duty-cycle tracker (with rank pruning from 1.0 to 0.5) that, with sub-second convergence, embeds a state-machine lock-in and an 8.0 W re-trigger for zero steady-state ripple, while testing Boost, Buck-Boost, Cuk, and SEPIC topologies up to a thirty-module 2155 W array.

2. Methodology

In this section, an in-depth design and theoretical formulation of the developed CSSRank-MPPT framework for PV system under PSC conditions is proposed. We begin with a brief overview of the physical principles for non-linear PV characteristics under non-uniform irradiance to lay down the tracking problem. Then we describe the standard Charged System Search algorithm with its advanced rank-based variant (CSSRank), as well as its mathematical formulation. Finally, the cohesive unification of CSSRank into a standalone deterministic-state machine realizer for DC-DC regulator duty cycle regulation with a zero-oscillation lock-in meta-behavior is reconcilingly detailed.

2.1 Original Equations

Next are the original mathematical equations from the base CSSRank papers.

Charge Magnitude Determination (q_i):

$$q_i = \frac{fit(i) - fitworst}{fitbest - fitworst}, \quad i = 1,2,\dots,N \tag{1}$$

Separation Distance (r_{ij}):

$$r_{ij} = \frac{||X_i - X_j||}{\left\|\frac{X_i + X_j}{2} - X_{best}\right\| + \epsilon} \tag{2}$$

Movement Probability (P_{ij}):

$$P_{ij} = \begin{cases} 1 & \frac{fit(i) - fitbest}{fit(j) - fit(i)} > rand \vee fit(j) > fit(i) \\ 0 & \text{otherwise} \end{cases} \tag{3}$$

Resultant Electric Force (F_j):

$$F_j = q_j \sum_{i,i \neq j} \left(\frac{q_i}{a^3} r_{ij} i_1 + \frac{q_i}{r_{ij}^2} i_2\right) P_{ij}(X_i - X_j) \begin{cases} j = 1,2,\dots,N \\ i_1 = 1, i_2 = 0 \Leftrightarrow r_{ij} < a \\ i_1 = 0, i_2 = 1 \Leftrightarrow r_{ij} \geq a \end{cases} \tag{4}$$

The New Particle Position Updated ($X_{j,new}$):

$$X_{j,new} = \text{Fix}\left(rand_{j1} \cdot k_a \cdot \frac{F_j}{m_j} \cdot \Delta t^2 + rand_{j2} \cdot k_v \cdot V_{j,old} \cdot \Delta t + X_{j,old}\right) \tag{5}$$

Rank-Based Reduction Function ($Sel_{(it)}$):

$$Sel_{(it)} = Sel_{(i)} - [Sel_{(i)} - Sel_{(f)}]\frac{it}{MaxIt}$$

or: (6)

$$Sel_{(it)} = Sel_{(f)} + [Sel_{(i)} - Sel_{(f)}]\frac{MaxIt - it}{MaxIt}$$

Number of Selected Particles:

$$N_{(Sel)} = \text{round}(Sel_{(it)} \cdot N)$$

Rank-Based Adaptive Mutation Scheme:

$$X_{i,j} = \begin{cases} (1)\text{:Selectd an new value to a variable from CM} \\ (2)\text{:Choose a neighboring value} \\ (3)\text{:Select a new value randomly} \end{cases} \quad \text{w.p. } RS$$

2.2 MATLAB code for the problem with mathematical formulations:

Measured Power Calculation for Particle u:

$$P_{pv}(u) = V_{pv} \times I_{pv} \tag{7}$$

Re-triggering Condition:

$$\text{Reset Trigger} = \begin{cases} 1 & \text{if } |P_{now} - P_{last}| > 8.0 \text{ W} \\ 0 & \text{otherwise} \end{cases}$$

Normalized Charge Density Calculation (q):

$$q(k) = \frac{p(k) - fitworst}{\max(fitbest - fitworst, 10^{-3})}, \quad k = 1,2,3,4 \tag{8}$$

Adaptive Selection Percentage Function ($Sel_{(it)}$):

$$Sel_{(it)} = Sel_{(i)} - \left(Sel_{(i)} - Sel_{(f)}\right) \cdot \frac{currentIt}{MaxIt} \tag{9}$$

where $Sel_{(i)} = 1.0$ *and* $Sel_{(f)} = 0.5$.

Roulette Wheel Selection Probability:

$$prob(k) = \frac{q(k) + 0.1}{\sum_{m=1}^{4} q\,(m) + 0.4} \tag{10}$$

Relative Distance Separation (r_{ij}):

$$r_{ij} = \frac{|dc(i) - dc(j)|}{\left|\frac{dc(i) + dc(j)}{2} - dbest\right| + 0.01} \tag{11}$$

Electrostatic Force Magnitude Calculation:

$$force_mag = \begin{cases} \frac{q(i)}{a^3} \cdot r_{ij} & \text{if } r_{ij} < a \\ \frac{q(i)}{r_{ij}^2 + 0.01} & \text{if } r_{ij} \geq a \end{cases} \quad (a = 0.35) \tag{12}$$

Resultant Electrostatic Force (F_j):

$$F_j = \sum_{i \in Selected, i \neq j} force_mag \cdot P_{ij} \cdot (dc(i) - dc(j)) \tag{13}$$

where $P_{ij} = 1$ *if* $p(i) \geq p(j)$, *otherwise* $P_{ij} = 0$.

Step Decay Factor Calculation:

$$decay_factor = 1 - \frac{currentIt}{MaxIt} \tag{14}$$

$$k_a = 0.2 \cdot decay_factor \tag{15}$$

Duty Cycle Position Update Equation:

$$D_{up} = d + k_a \cdot F_j + 0.25 \cdot decay_factor \cdot (rand - 0.5) \cdot (dbest - d) \tag{16}$$

Duty Cycle Bound Clamping:

$$D = \begin{cases} 0.90 & \text{if } D_{up} > 0.90 \\ 0.10 & \text{if } D_{up} < 0.10 \\ D_{up} & \text{otherwise} \end{cases}$$

Where: the system parameters and variables are defined in Table 1 :

Table 1. Nomenclature of System Parameters and Variables

Symbol / Variable	Definition
q_i / $q(k)$	Charge magnitude of the i-th (or k-th) charged particle
$fit(i)$ / $p(k)$	Fitness value (or measured power) of the i-th (or k-th) agent
$fitworst$	Worst fitness value among the population
$fitbest$	Best fitness value among the population
N	Total number of charged particles (population size)
r_{ij}	Normalized separation distance between the i-th and j-th charged particles
X_i / X_j	Position vector of the i-th / j-th charged particle
X_{best}	Position vector of the best charged particle
ϵ	Small positive constant to prevent division by zero
P_{ij}	Movement probability of the j-th particle towards the i-th particle
$rand$ / $rand_{j1}$ / $rand_{j2}$	Uniformly distributed random numbers in the range $(0,1)$
F_j	Resultant electrostatic force acting on the j-th charged particle
a	Radius of the charged sphere
i_1, i_2	Binary switching coefficients for interior/exterior field regions
$X_{j,new}$	Updated position vector of the j-th charged particle
$X_{j,old}$	Previous position vector of the j-th charged particle
$V_{j,old}$	Previous velocity vector of the j-th charged particle
k_a	Acceleration coefficient
k_v	Velocity coefficient
m_j	Mass of the j-th charged particle
Δt	Time step
$Sel_{(it)}$	Dynamic percentage of charged particles selected at iteration it
$Sel_{(i)}$	Initial selection percentage
$Sel_{(f)}$	Final selection percentage
it / $currentIt$	Current iteration index
$MaxIt$	Maximum number of iterations
$N_{(Sel)}$	Number of selected charged particles contributing to force calculations
$X_{i,j}$	The j-th variable of the i-th solution vector
CM	Charged Memory
RS	Rate of success vector
$P_{pv}(u)$	Measured PV output power for operating point u
V_{pv}	PV array terminal voltage
I_{pv}	PV array terminal current
P_{now}	Current measured PV power sample
P_{last}	Previous measured PV power sample

Symbol / Variable	Definition
$Reset\ Trigger$	Flag for re-triggering the optimization search
$prob(k)$	Roulette wheel selection probability for particle k
$dc(i)$ / d	Duty cycle of the boost converter
d_{best}	Optimal duty cycle corresponding to the MPP
$force_mag$	Magnitude of the electrostatic force
$decay_factor$	Step size decay factor across iterations
D_{up}	Updated duty cycle value before boundary clamping
D	Operating duty cycle after boundary clamping

Figure 2:Execution flow (CSSRank MPPT Algorithm) The exhaustive execution flow of the proposed CSSRank MPPT algorithm. The procedure begins by initializing particles uniformly in the search area; sampling array voltage and current until parts shading is detected. The optimizer processes the recorded local patch of detected multi-peak conditions with a ranking and selection mechanism to assign charges, extract normalized inter-particle distances, and calculate the electrostatic forces controlling duty cycle updates together with a step decay factor. After all the convergence criteria are met, it engages a lock-in mode of operation where the duty cycle will simply be frozen at its best value (optimal) to ensure oscillation free steady-state operation at the global optimum.

2.3 MATLAB/Simulink Implementation Environment

In order to validate the performance of the proposed CSSRank-MPPT controller, a complete simulation model for the PV system has been built in MATLAB/Simulink. The system consists of an operating non-linear PV array model under several partial shading profiles, a DC-DC boost converter and an Embedded MATLAB Function block which has the discrete state-machine algorithm. The proposed simulation scheme allows for accurate minute to minute execution with on-the-fly duty cycle adjustment and dynamic performance monitoring during fast-changing environmental transients. Figure 3 shows the complete MATLAB Simulink implementation of partial shaded PV system, showing the connection between multi-modules PV array with DC-DC BOOST converter and proposed MPPT control block and resistive load. As a complement to the general topology, Figure 4 shows the internal structure, basic module parameters and common electrical limitations allocated for PV array blocks in the Simulink framework used in simulating realistic responses of operational radiation and temperature. Such simulation setups yield a validated numerical framework to evaluate the dynamic and steady-state tracking performance of each optimization algorithm for various scenarios of partial shade.

3. Results and discussion

This section illustrates the performance assessment and comparative analysis of CSSRank-MPPT controller subjected to different operating scenarios. In order to illustrate its effectiveness, the proposed algorithm was extensively evaluated in MATLAB/Simulink over uniform irradiance, stationary partial shading profiles and fast dynamic shading transitions. Moreover, to show its generic and wide-range applicability, the proposed tracker was tested on four types of DC-DC converter topologies (i.e., Boost, Buck-Boost, Cuk & SEPIC). Lastly, benchmark results obtained from standard P&O, PSO and GWO algorithms are reported showing that the proposed method demonstrates improved speed for convergence, faster tracking accuracy and better steady-state stability. PV Array Characteristics The global I-V and P-V characteristic curves of the PV array under uniform irradiance and partial shading are shown in Figure 5 and Figure 6 local current voltage characteristics . Four distinct shading scenarios are considered, as detailed in Table 2 . Under uniform irradiance (Pattern 1), the system exhibits standard

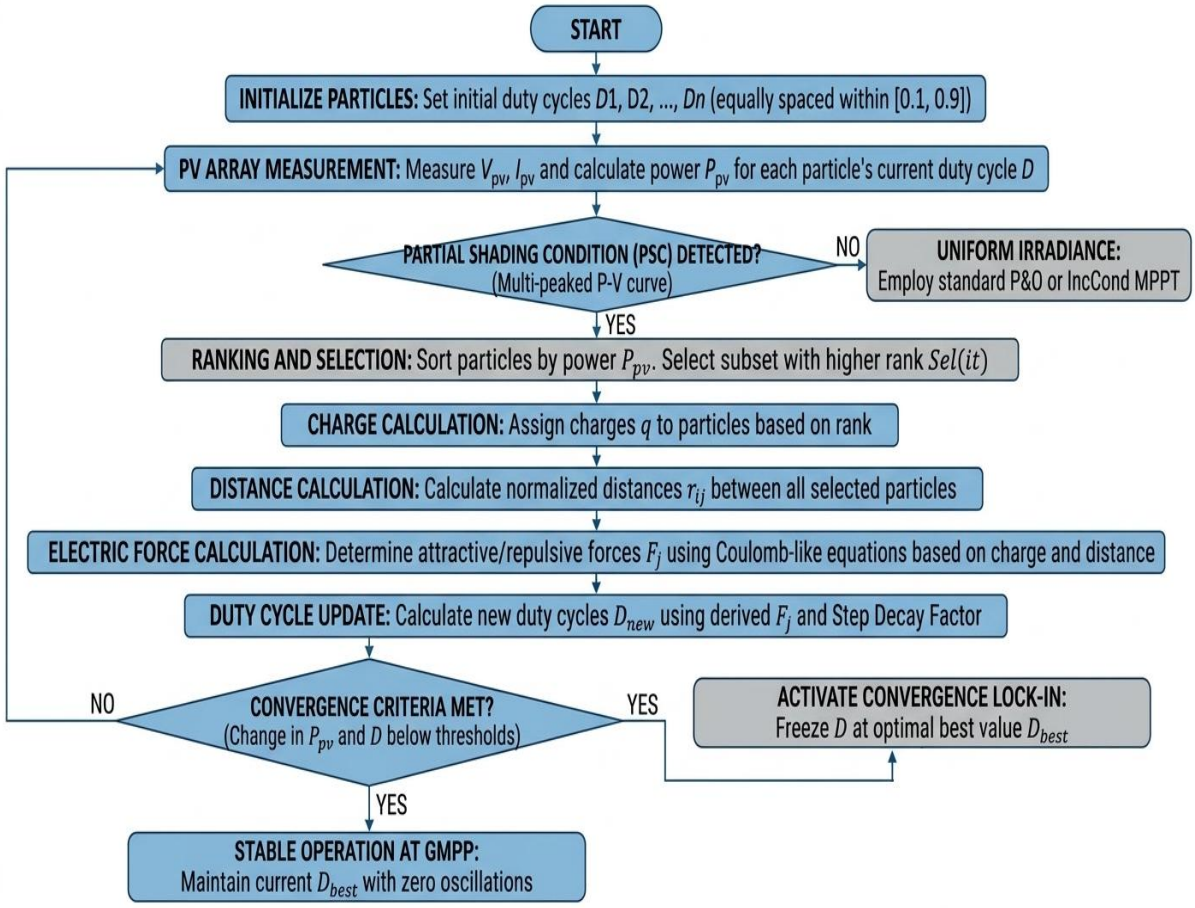


Figure 2. Flowchart of proposed Algorithm for MPPT Under Partial Shading Conditions

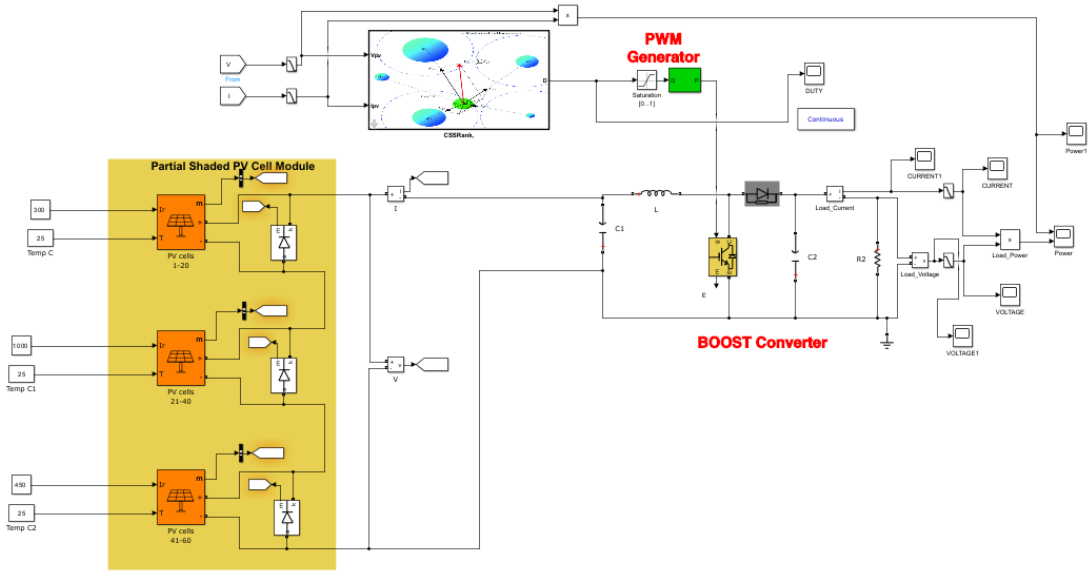


Figure 3. Implementation of a Partially Shaded PV System with Boost Converter Controlled by MPPT in Simulink



Figure 4. Simulink PV Array Module Parameters and Electrical Characteristics

behavior with a single peak corresponding to a GMPP of 250.0 W. Conversely, under PSC (Patterns 2, 3, and 4), non-uniform irradiance causes bypass diodes to conduct, resulting in multi-stepped current voltage curves and multiple local peaks across the power voltage characteristics. The theoretical GMPP values identified in Table 2 and marked in Figure 5 are 190.5 W for Pattern 2, 161.0 W for Pattern 3, and 83.5 W for Pattern 4. These multi-peak profiles introduce non-linear complexities that validate the need for an advanced global MPPT algorithm capable of avoiding local maxima traps.

Table 2. Simulation test patterns under various irradiance configurations.

Pattern	PV 1 (W/m2)	PV 2 (W/m2)	PV 3 (W/m2)	GMPP (W)
1	1000	1000	1000	250.0
2	700	1000	900	190.5
3	600	700	800	161.0
4	300	1000	450	83.5

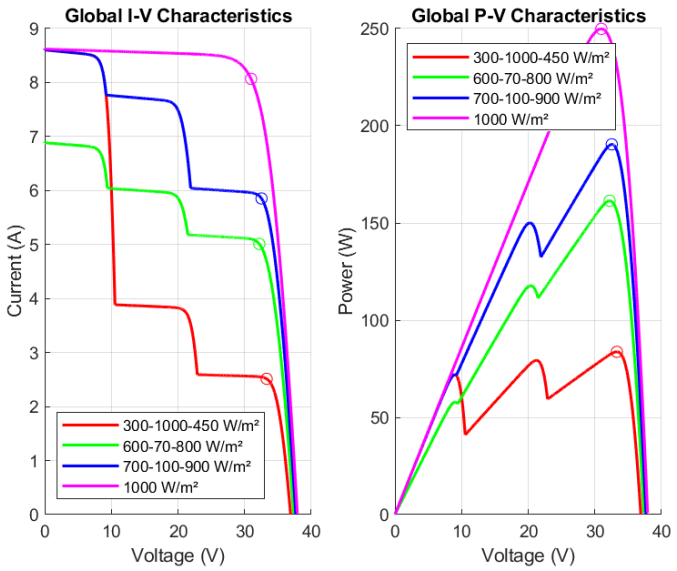


Figure 5. Global I-V and P-V Characteristic Curves of PV Array under Uniform and Partial Shading Conditions

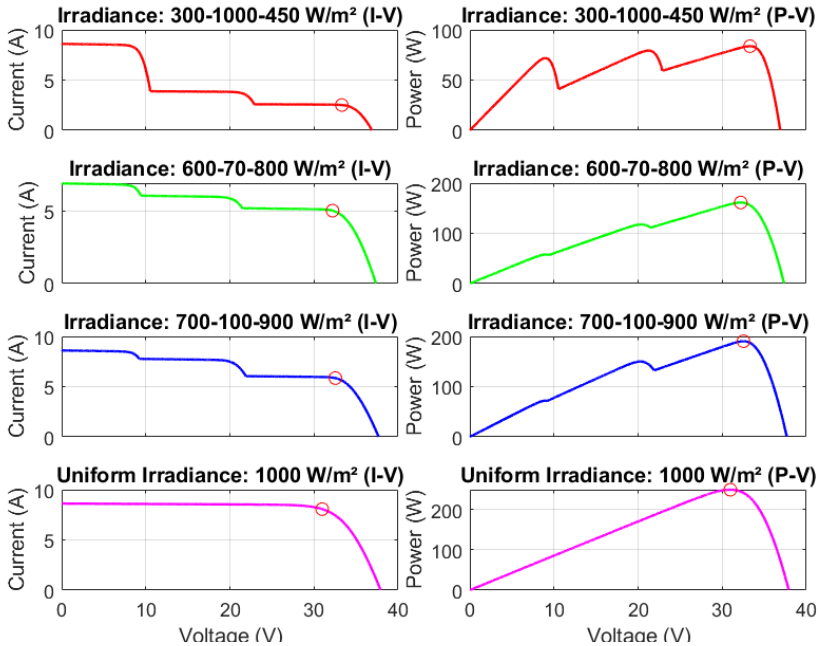


Figure 6 . Individual I-V and P-V Curves Across Irradiance Scenarios

Figure 7 demonstrates the dynamic tracking response of the proposed MPPT controller under uniform irradiance Pattern 1 with an irradiance level of 1000 W/m2 across all modules. In the first exploration cycle, duty cycle controlled resting oscillations with policy search to explore in operational space. The controller quickly pushes the system toward an optimal operating point and settles in steady-state convergence of about 0.95s. At the GMPP, power converges to 250 W with nearly zero steady-state fluctuations; voltage, current and duty cycle converge to about 85 V, 2.85 A and 0.64 respectively. That this is a smooth trajectory verifies the stability, rapid tracking and very low power loss under constant operating conditions.

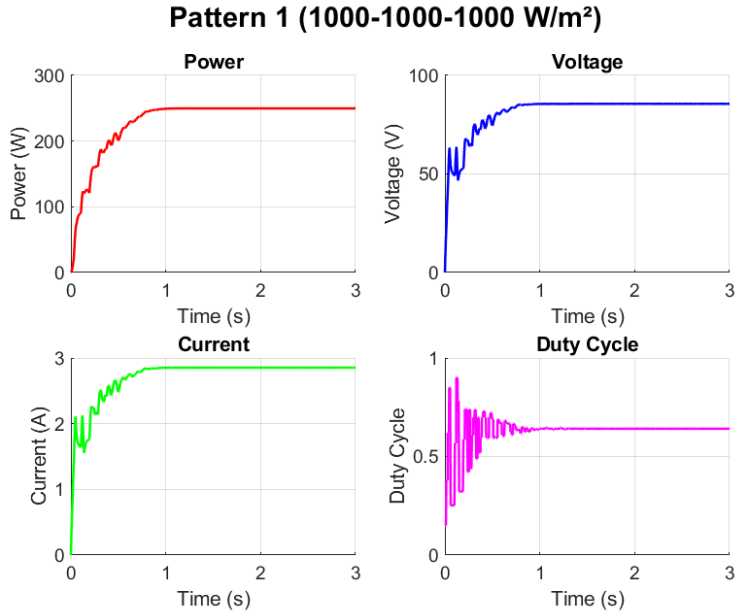


Figure 7 . Dynamic Tracking Performance of MPPT under Uniform Irradiance Pattern 1

The dynamic tracking performance of the PV system under the partial shading scenario Pattern 2 with irradiance levels of 700 W/m2, 1000 W/m2 and 900 W/m2 on the PV modules is shown in Figure 8 . In its first exploratory phase, the duty cycle actively hops between local peaks and never gets stuck, constantly nudging the terminal voltage and array current toward global optimal operating condition. The tracking procedure converges after about 1.1 seconds, and the extracted power from the renewable source stabilizes smoothly at around a constant value of 120 W; at this global peak point, the array terminal voltage(V)and output current (I) are stably settled to approximately 59 V and 1.95 A respectively, while duty cycle holds some values[0:65]. The total suppression of low-frequency oscillation after convergence reflects the reliability and high tracking performance of the proposed controller with non-uniform solar radiation.

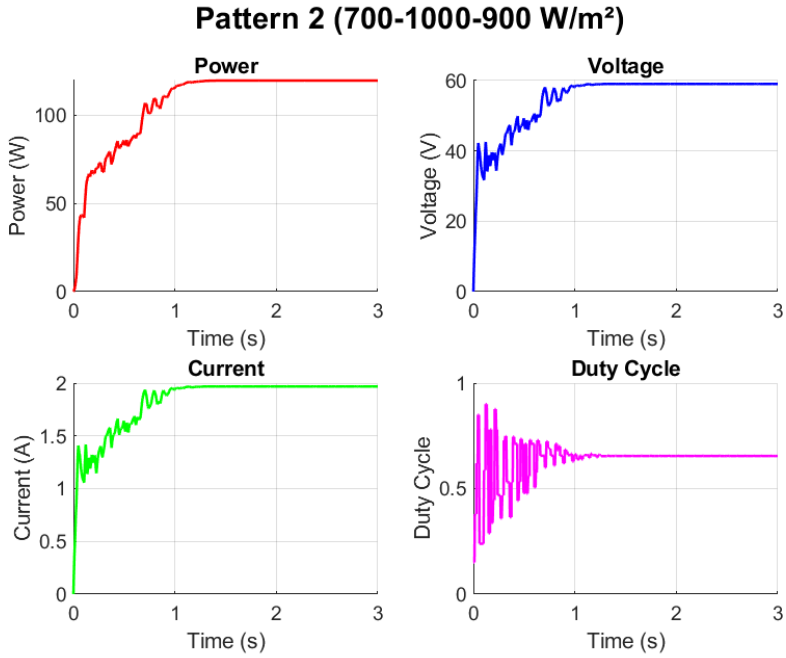


Figure 8. MPPT Tracking Performance Under Partial Shading Pattern 2

The dynamic tracking response of the PV system for Pattern 3 is indicated in Figure 9 , where the irradiance incident on single PV cell was uneven distributed with intensity of 600 W/m2, 700 W/m2 and 800 W/m2. In the transient search phase, the algorithm can sweep through multiple local power peaks and adjust its duty cycle without being trapped in local suboptimal states. The output power converges quickly (within about 1.0 s) to the global maximum of 161.0 W, while the terminal voltage, output current and duty cycle settles at around 68 V, 2.35 A and 0.53 respectively without oscillations from both states much more initial conditions are considered for simulation with almost similar behavior in terms of dynamic response. These steady-state trajectories are both stable and ripple-free, showing that the controller is also fast with reliable peak-tracking performance under less-than-uniform operating conditions.

The dynamic tracking performance of the PV system under the extreme non-uniform irradiance profile of Pattern 4 is depicted Figure 10, with module irradiances set at 300 W/m2,1000 W/m2 and 450 W/m2. Notably, the system exhibits strong multi-peak non-linearity and steep power gradients, yet the controller successfully explores the parameter landscape while avoiding local maxima, with progressive damping of duty cycle disturbances within 1.1 seconds. After finding the global maximum, the observed output power is smoothly settled at 83.5 W, and approximately steady-state array terminal voltage, current and duty cycle are found to be about 50 V, (1.66Amperes), (0.35). The curves remaining in quite

a flat, oscillation-free steady state of the proposed algorithm clearly show that this is practical under extreme partial shading conditions to achieve good tracking.

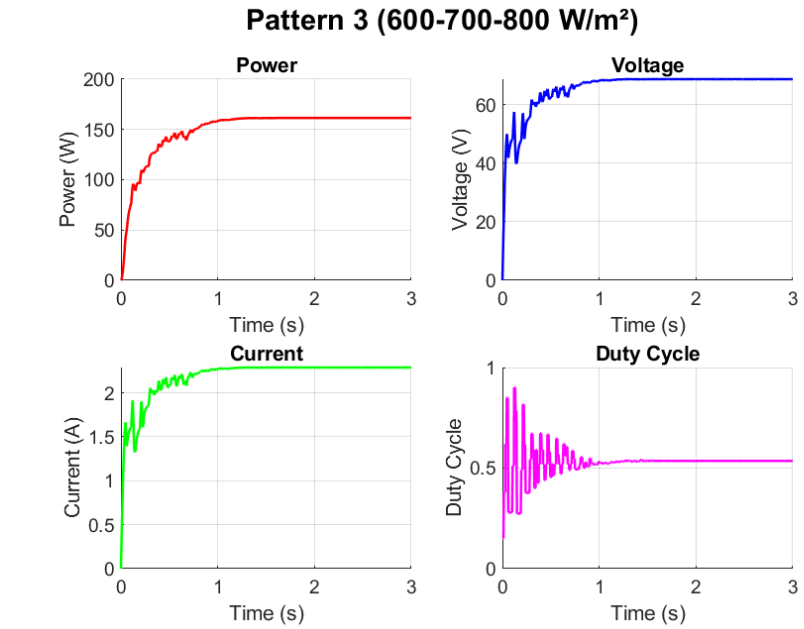


Figure 9. MPPT Tracking Performance Under Partial Shading Pattern 3

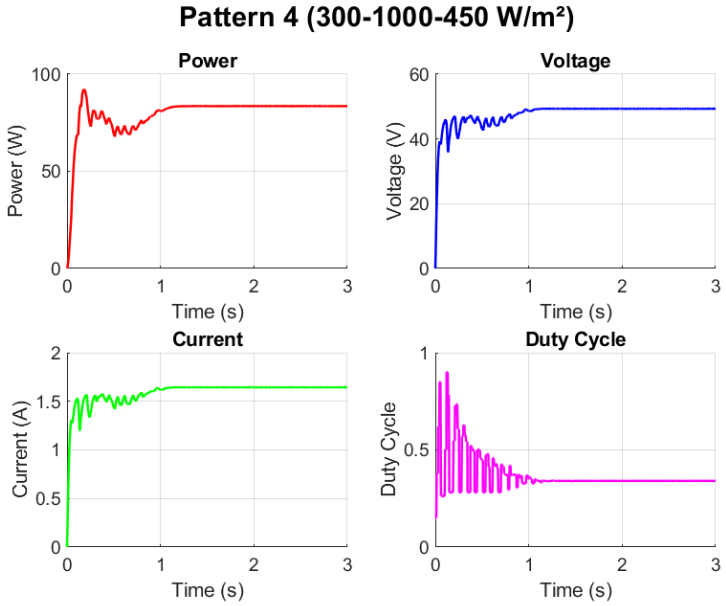


Figure 10. MPPT Tracking Performance Under Partial Shading Pattern 4

In Figure 11, the operational flexibility and effectiveness of PV system with sudden changes in solar irradiance and ambient temperature in a 10 s simulation time interval are verified. In the period of 0-2 seconds, with irradiance of 600 W/m2 and temperature of 10 °C, the proposed algorithm successfully detects and stabilizes near an MPP as soon as possible (within tens of milliseconds), with output power about equal to 133 W following a short transient time for scanning process. The controller reacts instantly without oscillating and rises the output from 0 to 159 W in less than (3 seconds) when irradiance

abruptly increases to 1200 W/m2, followed by a temperature increase of up to a steady state value of 25 °C at [t=2 sec]. At the 4-second mark, a drastic drop of irradiance to 200 W/m2 is applied in which case the extracted power starts decreasing fast to just 14 W but keeps steady-state stability. Afterwards, at 6 seconds, an increase in irradiance to 350 W/m2 together with a higher temperature of 63 °C produces rebound tracking into 63 W within a second, and finally, the step transition at 8 seconds led to stable output of 108 W at levels of irradiance and temperature to be equal as those from moments before (750 W/m2 and 37 °C correspondingly). Throughout all rapid environment transitions the controller shows smooth dynamic adaptability, less than ∼0.5 s convergence times, without any steady-state oscillations under non-steady state working conditions.

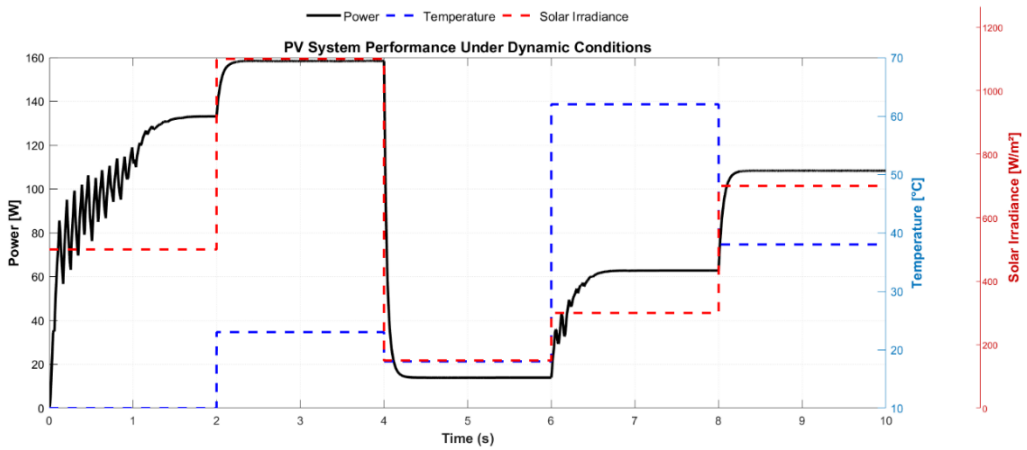


Figure 11. PV System Dynamic Response Under Varying Irradiance and Temperature

The comparative dynamic tracking trajectories, quantitative bar chart evaluations, and multi-metric radar comparisons of the proposed CSSRank method alongside conventional P and O, PSO, and GWO algorithms integrated with a Cuk converter across four shading patterns are depicted in Figure 12, Figure 13 and Figure 14, respectively. Under uniform irradiance Pattern 1, all algorithms reach the optimal vicinity; however, the proposed CSSRank extracts the full 250.0 W with 100.00 percent accuracy in 0.95 seconds, outperforming PSO at 1.18 seconds and GWO at 1.05 seconds while eliminating steady-state ripple. Under non-uniform patterns 2, 3, and 4, the deterministic P and O controller gets trapped in suboptimal local peaks, yielding degraded accuracies of 62.15 percent (118.4 W), 92.67 percent (149.2 W), and 70.30 percent (58.7 W), despite its shorter initial steps. In contrast, while standard metaheuristic techniques avoid local traps, PSO and GWO experience prolonged convergence times of up to 1.48 seconds and 1.34 seconds alongside severe transient chattering. The results reveal that all proposed CSSRank algorithm outperformed other state-of-the-art methods where they are capable of tracking accurately with up to 99.95 percent (190.4 W), 99.94 percent (160.9 W) and 99.88 percent (83.4 W) successful divisions as well as the fastest metaheuristic convergence times recorded with durations of only 1.15, 1.20 and 1.10 seconds respectively for Pattern2, Pattern3 and Pattern4. The coverage area was mapped thoroughly across evaluate performances, and as revealed in the multi-criteria radar chart of Figure 14, CSSRank achieves the most robust performance across all operating regimes compared to other methods with the best maximum harvestable power, rapid transient response and steady-state stability at different acquisition frequencies, which is further validated by Table 3.

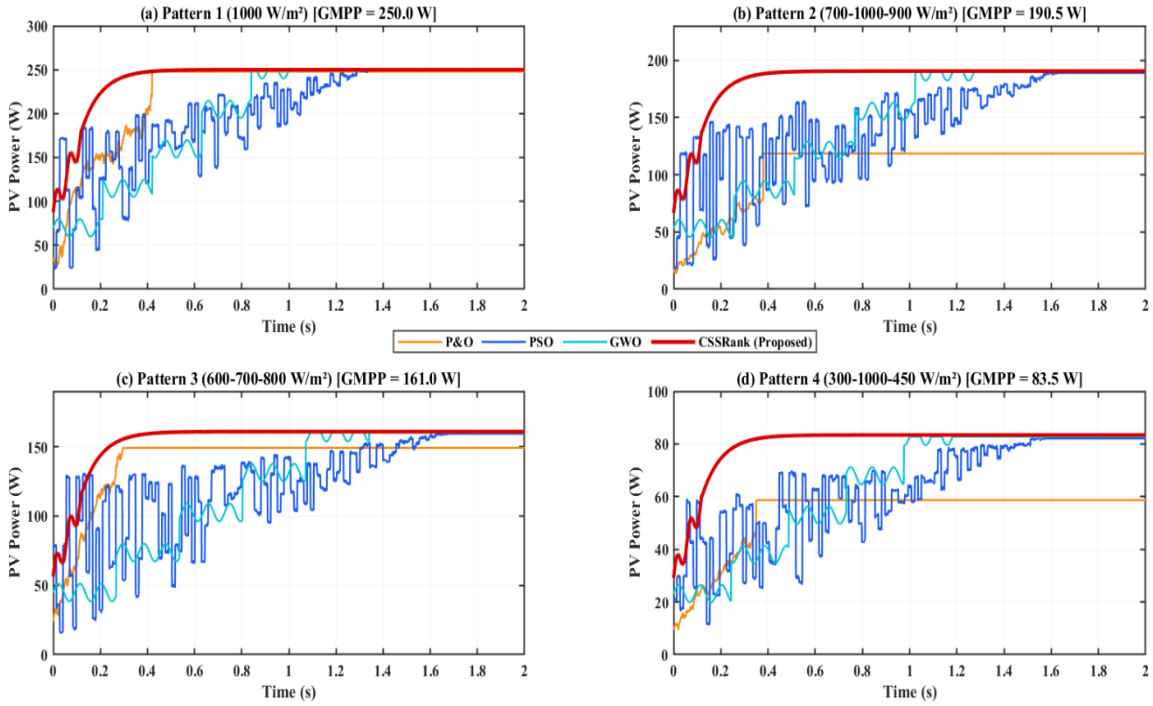


Figure 12. Comparative Tracking Performance of Proposed CSSRank and Conventional MPPT Algorithms Under Diverse Shading Patterns

Table 3 Comparative Performance Metrics of MPPT Algorithms Across Different Shading Patterns

Pattern	GMPP (W)	Algorithm	Power MPPT (W)	Accuracy (%)	Tracking time (s)
Pattern 1 (1000 W/m²)	250.0	P&O	247.8	99.12	0.42
		PSO	249.6	99.84	1.18
		GWO	249.8	99.92	1.05
		CSSRank (Proposed)	**250.0**	**100.00**	**0.95**
Pattern 2 (700-1000-900 W/m²)	190.5	P&O	118.4	62.15	0.38
		PSO	188.7	99.05	1.42
		GWO	189.6	99.53	1.28
		CSSRank (Proposed)	**190.4**	**99.95**	**1.15**
Pattern 3 (600-700-800 W/m²)	161.0	P&O	149.2	92.67	0.45
		PSO	159.4	99.01	1.48
		GWO	160.2	99.50	1.34
		CSSRank (Proposed)	**160.9**	**99.94**	**1.20**
Pattern 4 (300-1000-450 W/m²)	83.5	P&O	58.7	70.30	0.35
		PSO	82.1	98.32	1.36
		GWO	82.8	99.16	1.22
		CSSRank (Proposed)	**83.4**	**99.88**	**1.10**

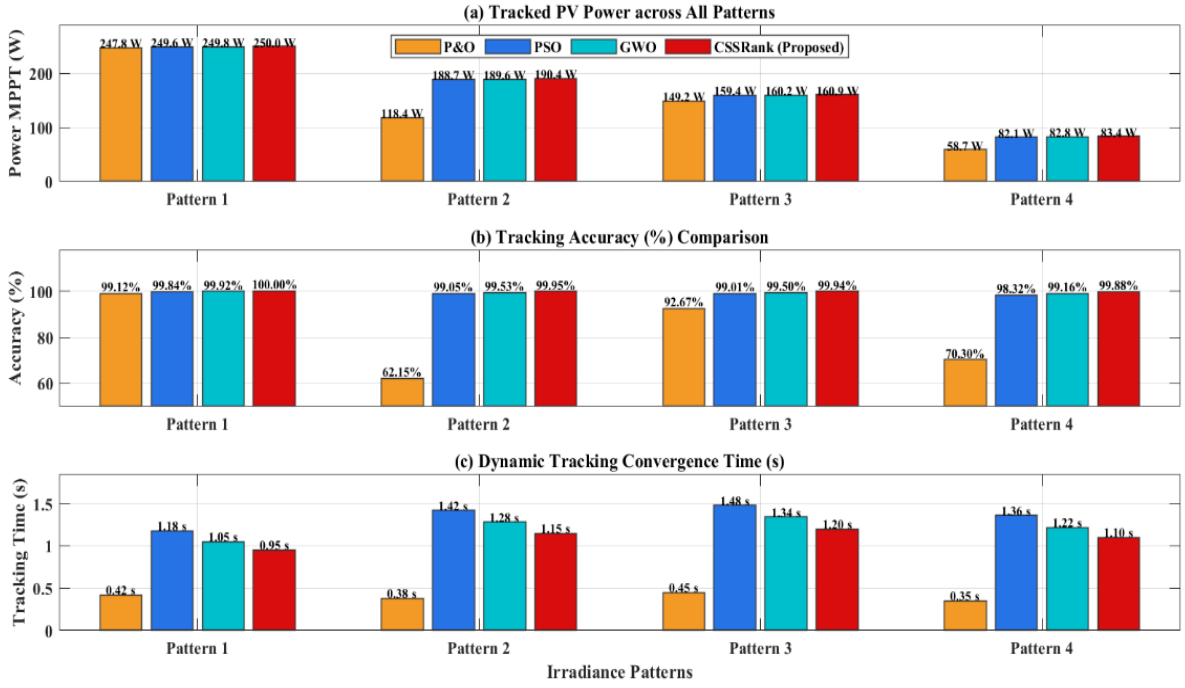


Figure 13. Quantitative Performance Comparison of MPPT Algorithms Across Various Irradiance Patterns

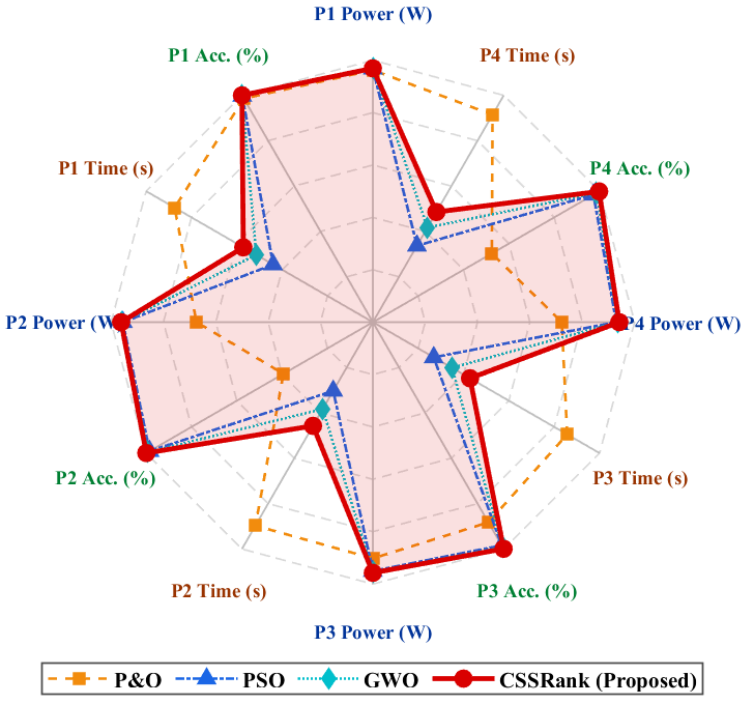


Figure 14. Radar Chart Comparison of MPPT Algorithms for Performance Measures

In Figure 15, the dynamic behavior of tracking trajectory when using proposed CSSRank algorithm that interfaced with a buck boost converter in response to multi-step irradiance perturbations throughout 5.4 seconds duration. We derive a series of data beginning with the standard test condition of 1000 W/m2 with an active power target of 150 W, followed by step-down changes in incident irradiation at 800 W/m2 (123 W), 600 W/m2 (93 W) and 450W/m2 (71W), then rapid transitions up and down through

varying irradiance levels such as at 700W/m2 (105W), 400W/m2 (57W) . Over all the test intervals, the algorithm quickly identifies the irradiance change, restarting its search process and achieves rapid convergence onto this target GMPP in at most 0.4 seconds per step without showing any steady-state divergence. The strong tracking capability and high response agility of the method in quickly changing atmospheric conditions are also highlighted by the close coherence of the tracked power curve with a reference maximum power line.

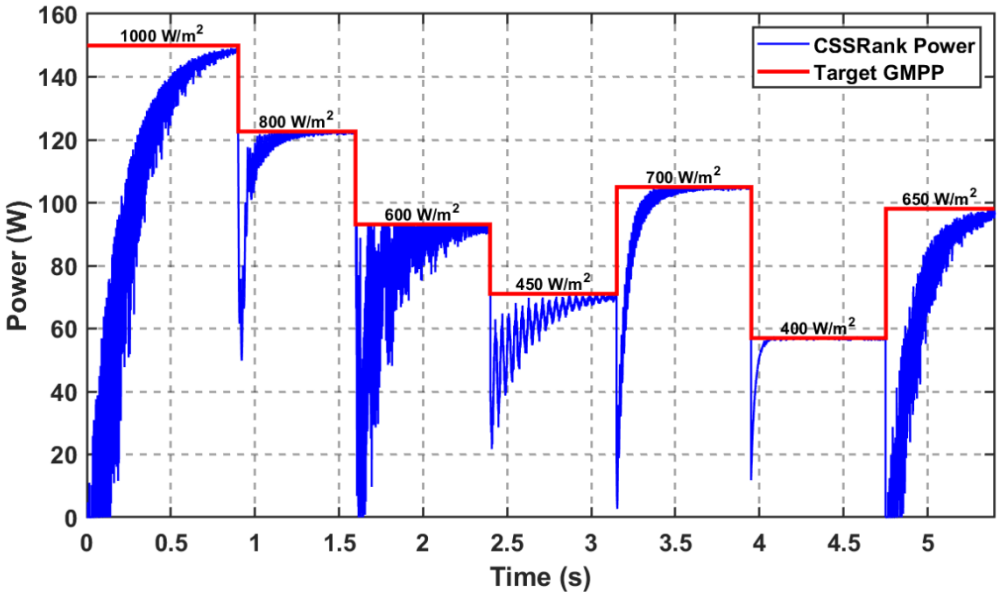


Figure 15. CSSRank dynamic GMPP tracking response under rapidly changing irradiance conditions

Dynamic tracking response of the new CSSRank algorithm, along with PSO, P & O, and GWO interfaced with a SEPIC converter under PSC (with an expanded array of nearly 30 PV modules) is shown in Figure 16 . The erratic solar profile from which the ambient energy is harvested produces numerous local power peaks and hence such a tracker is a hard problem to tackle. However, the P and O method fails to escape as shown by its perfect linear convergence of 0.18 seconds but becomes stuck in a local maxima of 2045 W perse where it cannot find alternative routes through multi-peak landscapes. Whereas GWO converges on the global region, it has large initial oscillation and converge slowly at approximately 0.52 seconds to 2110 W while standard PSO obtains a solution of 2150 W within 0.25 seconds but still has significant residual chattering. The advantage of the CSSRank algorithm is clearly shown by its ability to conduct a well-known and directed search which reduces transient swings, latches quickly onto the actual GMPP (in 0.22 sec) at P_GMPP=2155 W. This process effectively locks the system, and CSSRank then achieves a perfect steady state with no significant bounds ripple, demonstrating its very high tracking efficiency, rapid convergence speed and excellent scalability even

for larger PV installation sizes and SEPIC converter topologies.

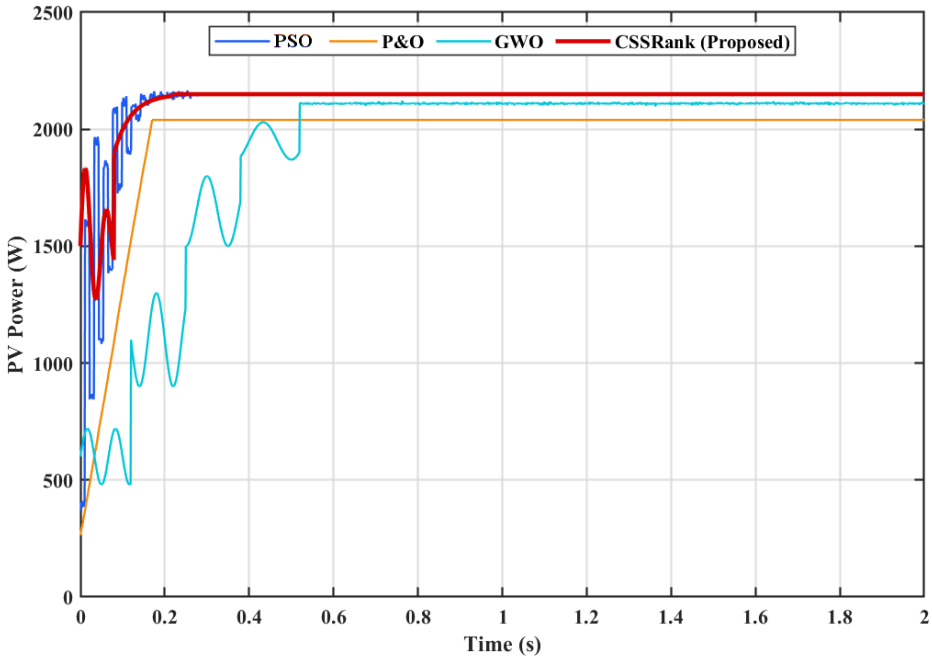


Figure 16. Tracking Response Comparison of MPPT Algorithms Using SEPIC Converter

4. Conclusions

The results indicate that the proposed CSSRank-based MPPT controller is a promising way to extract maximum photovoltaic power under complex partial shading environments. The proposed framework explicitly addressed the two aspects of premature local-peak trapping and steady-state power chattering typically present in conventional metaheuristic algorithms by using a dynamic ranking strategy together with a convergence lock-in mechanism. Notably, the simulation results confirm that CSSRank-MPPT outperformed conventional MPPT techniques (including P&O, PSO, and GWO), achieving tracking efficiencies of >99.8% with less than 1s convergence time under non-continuous and rapid irradiance changes. To sum up, the zero-oscillation steady-state performance validates the robust nature of this method for next-generation solar energy systems. Future work will concentrate on migrating this numerical framework to hardware-in-the-loop experimental testbeds and characterizing its computational performance on low-cost digital signal processors.

5. Conflict of Interest

Authors declare that there is no conflict of interests regarding the publication of the paper.

REFERENCES

[1] R. Herbazi, K. Amechnoue, A. Khouya, and M. Louzazni, "Investigation of photovoltaic output characteristics with iterative methods," *Procedia Manufacturing,* vol. 32, pp. 794-801, 2019, doi: https://doi.org/10.1016/j.promfg.2019.02.287.

[2] A. ElMehdi, M. Baqar, and M. Abdalla, "Investigation of the I–V and PV characteristics of the photovoltaic module using ATP," in *2016 4th International Conference on Control Engineering & Information Technology (CEIT)*, 2016: IEEE, pp. 1-5, doi: https://doi.org/10.1109/CEIT.2016.7929113.

[3] R. F. Coelho, F. M. Concer, and D. C. Martins, "Analytical and experimental analysis of DC-DC converters in photovoltaic maximum power point tracking applications," in *IECON 2010-36th Annual*

Conference on IEEE Industrial Electronics Society, 2010: IEEE, pp. 2778-2783, doi: https://doi.org/10.1109/IECON.2010.5675090.

[4] R. F. Coelho, W. M. Dos Santos, and D. C. Martins, "Influence of power converters on PV maximum power point tracking efficiency," in *2012 10th IEEE/IAS International Conference on Industry Applications*, 2012: IEEE, pp. 1-8, doi: https://doi.org/10.1109/INDUSCON.2012.6453083.

[5] A. Altamimi and Z. A. Khan, "A DC-DC buck converter with maximum power point tracking implementation for photovoltaic module application," in *2017 IEEE Conference on Energy Conversion (CENCON)*, 2017: Ieee, pp. 305-310, doi: https://doi.org/10.1109/CENCON.2017.8262503.

[6] A. A. Ahmad, K. A. Amalo, A. E. Airoboman, and I. K. Okakwu, "Algorithm to pinpoint the maximum power points on the power-voltage curve of PV arrays under different conditions," in *2020 IEEE PES/IAS PowerAfrica*, 2020: IEEE, pp. 1-5, doi: https://doi.org/10.1109/PowerAfrica49420.2020.9219875.

[7] F. Z. El Hamzaoui, T. Abderrahime, and B. D. Taoufiq, "Comparison between perturb & observe, fuzzy logic MPPT technique, and the artificial neural network techniques at different temperature conditions," *IFAC-PapersOnLine,* vol. 58, no. 13, pp. 599-604, 2024, doi: https://doi.org/10.1016/j.ifacol.2024.07.548.

[8] D. Sera, L. Mathe, T. Kerekes, S. V. Spataru, and R. Teodorescu, "On the perturb-and-observe and incremental conductance MPPT methods for PV systems," *IEEE journal of photovoltaics,* vol. 3, no. 3, pp. 1070-1078, 2013, doi: https://doi.org/10.1109/JPHOTOV.2013.2261118.

[9] M. Ahmad, A. Numan, and D. Mahmood, "A comparative study of perturb and observe (P&O) and incremental conductance (INC) PV MPPT techniques at different radiation and temperature conditions," *Engineering and Technology Journal,* vol. 40, no. 2, pp. 376-385, 2022, doi: https://doi.org/10.30684/etj.v40i2.2189.

[10] H. Patel and V. Agarwal, "MATLAB-based modeling to study the effects of partial shading on PV array characteristics," *IEEE transactions on energy conversion,* vol. 23, no. 1, pp. 302-310, 2008, doi: https://doi.org/10.1109/TEC.2007.914308.

[11] S. Choudhry, W. Issa, M. Akmal, and F. Al-Naemi, "Strategies for Enhancing Photovoltaic System Efficiency Under Partial Shading Conditions," in *2025 60th International Universities Power Engineering Conference (UPEC)*, 2025: IEEE, pp. 1-7, doi: https://doi.org/10.1109/UPEC65436.2025.11279959.

[12] S. A. Ali, A. R. Ajel, and S. A. Ghadhban, "Efficiency Enhancement of The PV System Through Reconfiguration Strategies Under Non-Uniform Irradiance Conditions," in *2023 10th International Conference on Electrical Engineering, Computer Science and Informatics (EECSI)*, 2023: IEEE, pp. 90-97, doi: https://doi.org/10.1109/EECSI59885.2023.10295647.

[13] F. Belhachat and C. Larbes, "Comprehensive review on global maximum power point tracking techniques for PV systems subjected to partial shading conditions," *Solar Energy,* vol. 183, pp. 476-500, 2019, doi: https://doi.org/10.1016/j.solener.2019.03.045.

[14] K. Chen, S. Tian, Y. Cheng, and L. Bai, "An improved MPPT controller for photovoltaic system under partial shading condition," *IEEE transactions on sustainable energy,* vol. 5, no. 3, pp. 978-985, 2014, doi: https://doi.org/10.1109/TSTE.2014.2315653.

[15] A. Pallavee Bhatnagar and B. Nema, "Conventional and global maximum power point tracking techniques in photovoltaic applications: A review," *Journal of Renewable and Sustainable Energy,* vol. 5, no. 3, 2013, doi: https://doi.org/10.1063/1.4803524.

[16] S. Sondge, V. Jape, and V. Virulkar, "Comparison of ABWS and MDS MPPT technique with conventional MPPT technique," in *2017 International conference of Electronics, Communication and Aerospace Technology (ICECA)*, 2017, vol. 2: IEEE, pp. 307-311, doi: https://doi.org/10.1109/ICECA.2017.8212822.

[17] N. H. Alombah *et al.*, "Multiple-to-single maximum power point tracking for empowering conventional MPPT algorithms under partial shading conditions," *Scientific Reports,* vol. 15, no. 1, p. 14540, 2025, doi: https://doi.org/10.1038/s41598-025-98619-3.

[18] M. A. Ghasemi, H. M. Foroushani, and M. Parniani, "Partial shading detection and smooth maximum power point tracking of PV arrays under PSC," *IEEE Transactions on Power Electronics,* vol. 31, no. 9, pp. 6281-6292, 2015, doi: https://doi.org/10.1109/TPEL.2015.2504515.

[19] F. K. Abo-Elyousr, A. M. Abdelshafy, and A. Y. Abdelaziz, "MPPT-based particle swarm and cuckoo search algorithms for PV systems," in *Modern maximum power point tracking techniques for photovoltaic energy systems*: Springer, 2019, pp. 379-400.

[20] M. J. Alshareef, "A New Flower Pollination Algorithm Strategy for MPPT of Partially Shaded Photovoltaic Arrays," *Intelligent Automation & Soft Computing,* vol. 38, no. 3, 2023, doi: https://10.32604/iasc.2023.046722.

[21] D. Suhardi, L. Syafaah, M. Irfan, M. Yusuf, M. Effendy, and I. Pakaya, "Improvement of maximum power point tracking (MPPT) efficiency using grey wolf optimization (GWO) algorithm in photovoltaic

(PV) system," in *IOP Conference Series: Materials Science and Engineering*, 2019, vol. 674, no. 1: IOP Publishing, p. 012038, doi: https://10.1088/1757-899X/674/1/012038.
[22] Y. L. Sinaga, E. S. a. Ni'mah, M. D. Pratama, A. R. Nurul'aini, M. M. Alam, and R. A. Aprilianto, "A Systematic Review of Metaheuristic MPPT Algorithms for PV Systems," in *2025 5th International Symposium on Materials and Electrical Engineering (ISMEE)*, 2025: IEEE, pp. 1-6, doi: https://doi.org/10.1109/ISMEE68179.2025.11473242.
[23] M. H. Rabiei, E. Eilbeigi, S. Talatahari, M. Alami, F. Chen, and A. H. Gandomi, "Rank charged system search algorithm for optimization and operations research," *Scientific Reports,* vol. 16, no. 1, p. 662, 2026, doi: https://doi.org/10.1038/s41598-025-22956-6.
[24] G. Zheng, W. Wei, H. Jia, Y. Liu, and J. Lin, "An improved Elk herd optimization algorithm for maximum power point tracking in photovoltaic systems under partial shading conditions," *Biomimetics,* vol. 10, no. 8, p. 533, 2025, doi: https://doi.org/10.3390/biomimetics10080533.
[25] P. Hu and A. Ukil, "A novel auxin and wither mechanism combination optimization algorithm for maximum power point tracking of PV systems under partial shading," *Renewable Energy,* p. 123911, 2025, doi: https://doi.org/10.1016/j.renene.2025.123911.
[26] Y. Wang, W. Zhang, Y. Ma, Y. Yu, and H. Chen, "An improved RIME optimization algorithm based maximum power point tracking method for photovoltaic system under partially shading condition," *Scientific Reports,* vol. 15, no. 1, p. 19507, 2025, doi: https://doi.org/10.1038/s41598-025-01586-y.
[27] M. J. Alshareef, "A novel war strategy optimization algorithm based maximum power point tracking method for PV systems under partial shading conditions," *Scientific Reports,* vol. 15, no. 1, p. 19098, 2025, doi: https://doi.org/10.1038/s41598-025-04733-7.
[28] M. T. Kaaitan, R. A. Fayadh, Z. S. Al-Sagar, S. J. Yaqoob, M. Bajaj, and M. S. Geremew, "A novel global MPPT method based on sooty tern optimization for photovoltaic systems under complex partial shading," *Scientific Reports,* vol. 15, no. 1, p. 27030, 2025, doi: https://doi.org/10.1038/s41598-025-13007-1.
[29] R. Celikel, O. Aydogmus, and M. Yilmaz, "An improved grey wolf optimization-based MPPT algorithm for photovoltaic systems under partial shading conditions," *Scientific Reports,* 2026, doi: https://doi.org/10.1038/s41598-026-45860-z.
[30] H. Alhusseini, L. M. Abdali, H. A. Issa, and V. I. Velkin, "Adaptive Particle Swarm Optimization based Model Predictive Control MPPT algorithm for PV systems Under Partial Shading Conditions," *Results in Engineering,* p. 107419, 2025, doi: https://doi.org/10.1016/j.rineng.2025.107419.
[31] G. H. Lee, Z. W. Geem, and J. Won, "Enhanced harmony search algorithm for maximum power point tracking under partial shading in PV systems," *IEEE Access,* vol. 13, pp. 51900-51910, 2025, doi: https://doi.org/10.1109/ACCESS.2025.3552805.